Langmuir

ARTICLE

pubs.acs.org/Langmuir

Long-Range Interaction between Heterogeneously Charged Membranes

Y. S. Jho,[*,†,‡] R. Brewster,[§] S. A. Safran,[∥] and P. A. Pincus[†,⊥]

[†]Materials Research Laboratory and [⊥]Departments of Physics and Materials, University of California at Santa Barbara, Santa Barbara, California, United States

[‡]WPI Advanced Institute for Materials Research, Tohoku University, Sendai 980-8577, Japan

[§]Division of Applied Science, California Institute of Technology, Pasadena, California 91125, United States

[∥]Department of Materials and Interfaces, Weizmann Institute of Science, Rehovot, Israel 76100

ABSTRACT: Despite their neutrality, surfaces or membranes with equal amounts of positive and negative charge can exhibit long-range electrostatic interactions if the surface charge is heterogeneous; this can happen when the surface charges form finite-size domain structures. These domains can be formed in lipid membranes where the balance of the different ranges of strong but short-ranged hydrophobic interactions and longer-ranged electrostatic repulsion result in a finite, stable domain size. If the domain size is large enough, oppositely charged domains in two opposing surfaces or membranes can be strongly correlated by the elecrostatic interactions; these correlations give rise to an attractive interaction of the two membranes or surfaces over separations on the order of the domain size. We use numerical simulations to demonstrate the existence of strong attractions at separations of tens of nanometers. Large line tensions result in larger domains but also increase the charge density within the domain. This promotes correlations and, as a result, increases the intermembrane attraction. On the other hand, increasing the salt concentration increases both the domain size and degree of domain anticorrelation, but the interactions are ultimately reduced due to increased screening. The result is a decrease in the net attraction as salt concentration is increased.

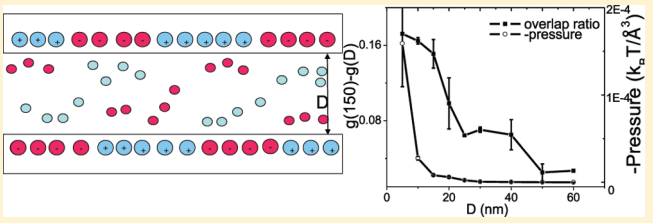

INTRODUCTION

Many aqueous systems of biological interest such as proteins or membranes comprising charged lipids are heterogeneously charged. In some cases, they can contain oppositely charged domains on two opposing, nearby surfaces. Although the net charge may be neutral in these systems, the charge distribution may be heterogeneous with a significant local net charge. This charge heterogeneity can play an important role in the interactions between two such surfaces that will depend strongly on the size and organization (correlations) of the charge domains.[1] Recently, efforts have been exerted to understand the interactions between surfaces bearing "patchy" charged domains.[2−7]

Patchy charged surfaces have been prepared experimentally[8−10] by coating a mica surface with a monolayer of a hydrophobic, cationic lipid; the polar groups are attached to the mica layer, and the chains extend away from the surface. Exposing such a treated surface to water in the absence of excess lipid causes roughly half of the lipid to "double over" and form a bilayer on the surface; AFM reveals irregular bilayer domains tens of nanometers in size. The finite-size domains of the cationic bilayer may be stabilized by the competition of the short-range line tension, which is responsible for the hydrophobic attraction, and the longer-ranged electrostatic repulsion of similarly charged lipids. These experiments measured a long-range attraction up to 60−80 nm nanometers between mica surfaces; the magnitude of the attraction is several orders of magnitude higher than expected from van der Waals interactions.

A theoretical analysis[6,11] of the problem showed that on a single surface, nanometer-sized domains should form due to the competing interactions. The theory predicts a first-order phase transition between finite-sized charged domains and macroscopic domains when either the salt concentration or the line tension exceeds a critical value. In addition, the interactions between two such patchy surfaces have also been studied.[11] Reference 5 suggests that in the weakly charged, Debye−Huckel (DH) regime, the addition of salt can actually increase the attractive interactions between surfaces. This counterintuitive result stems from the increased interaction strength of larger correlated domains (the domain size in the presence of relatively high salt is inversely related to the screening length) which more than compensates for the additional electrostatic screening between domains.

These theories[5] assume that charged domains on opposite surfaces or membranes are perfectly anticorrelated (with positive domains above negative ones), which presupposes rapid equilibrium of the domain size as the surface separation changes. As such, the interactions depend on the domain size and salt concentration. In this paper, we investigate the interactions of two patchy charged surfaces using particle simulations without assuming anything about their correlations. We predict the

Received: December 20, 2010
Revised: February 16, 2011
Published: March 16, 2011

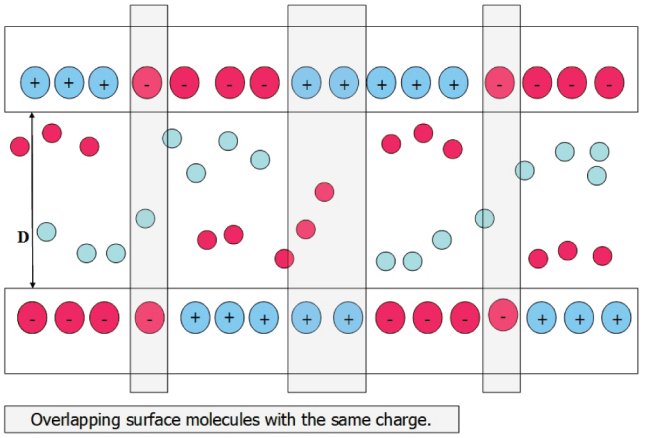

Figure 1. Side view of the system configuration. Light blue circles are positive ions, and light red circles are negative ions. The gray regions indicate the overlap of similarly charged surface molecules. The distance between charged surface is D.

magnitude and range of the long-range attraction between heterogeneously charged membranes as a function of the domain size and their degree of anticorrelation.

These molecular simulations depend on various assumptions regarding the form and magnitude of molecular interactions. We find that the domain size can be sensitive to both the form of the short-range potential and its magnitude, both of which can modify the line tension. Larger domains are formed on surfaces with smaller surface charge densities since the line tension dominates the electrostatic repulsion. However, in contrast to the domain size, the attractive pressure is reduced for smaller bare surface charge density. This suggests that increasing domain size does not necessarily imply larger attractive pressure. A similar trend is seen in our simulations when the salt concentration is varied. Higher salt resulted in larger domains consistent with theory, but the attractive pressure decreased as the salt concentration increased.[5,6]

This paper is organized as follows: In section II, we describe the system and the simulation method. This is followed in section III by the simulation results under various conditions of surface charge density and salt. We discuss and summarize the physical meaning of the results in section IV.

SIMULATION

We performed Monte Carlo simulations to study the interaction between two heterogeneously charged planes.[12] The system exhibits two-dimensional periodicity in directions parallel to the membranes but is finite in the normal direction. We assume for simplicity that the membranes are perfectly flat. The charged particles are modeled as hard spheres with the charge concentrated at the center. The configuration of the system is shown in Figure 1. In the experiments the positively and negatively charged domains[8,9] are associated with regions of bare mica, with a negative surface charge, and lipid bilayer patches, with positive surface charge. In our simulations, we model these patchy charged domains by surface-bound spheres of both positive charge (representing areas of lipid bilayer) and negative charge (representing areas of bare mica). The charges are confined to a fixed plane on the bilayer but are allowed to dynamically rearrange by motion along the surface. The molecules that constitute the mica surface are modeled as charged, hard spheres, while the charged lipid molecules are modeled as charged, cohesive molecules with a cohesion energy to account for the tail interactions of lipid molecules. This cohesion energy is responsible for the positive line tension between the lipid and mica domains (in the absence of electrostatic effects).

Table 1. Parameters Used

symbol	meaning
σ	diameter of a charged particle
σ_s	bare surface charge density
$\vec{r}_{ij}$	vector distance between particle i and j
ε	dielectric constant of the system
ε_{att}	coefficient of attractive part of nonelectrostatic potential
ε_{rep}	coefficient of repulsive part of nonelectrostatic potential
κ^{-1}	inverse screening length
l_B	Bjerrum length
R	domain size
D	separation of membranes
g	overlap ratio

We typically chose values of $\pm e$ for the positive and negative surface particles with the constraint that the surface remains macroscopically neutral. The bulk aqueous phase that separates the two patchy charged surfaces contains salt ions that are free to move in all three dimensions. The grand canonical Monte Carlo simulation method is applied with a constraint of constant salt chemical potential.[13] The chemical potential is calculated from the 3D periodic canonical ensemble simulation using a modified inverse Widom's method.[14−17] To maintain charge neutrality in the aqueous phase, a neutral set of positive and negative salt ions is selected together at every trial step; in our case, we insert or delete a set of both one positive and one negative salt particle at each step.

Our simulations were done with two plausible forms for the nonelectrostatic part of the interactions between the surface lipids that are not simple spherical molecules. We thus consider effective interactions between the lipids that depend only on the spacing of their centers. The interactions were modeled either as Lennard-Jones (LJ) interactions[18]

$$U_{LJ} = -\varepsilon_{att}\left(\frac{\sigma}{|\vec{r}_i - \vec{r}_j|}\right)^6 + \varepsilon_{rep}\left(\frac{\sigma}{|\vec{r}_i - \vec{r}_j|}\right)^{12}$$

or by an anisotropic alignment potential (Aln) (whose repulsive part is identical with the LJ interaction) as suggested by Brown[19]

$$U_{Aln} = -\varepsilon_{att}\left(\frac{\sigma}{|\vec{r}_i - \vec{r}_j|}\right)^2 + \varepsilon_{rep}\left(\frac{\sigma}{|\vec{r}_i - \vec{r}_j|}\right)^{12} \quad (1)$$

where σ is the diameter of a sphere and $\vec{r}_{ij}$ is the vector that specifies the vector distance between particles i and j. We will compare the results of these two different interaction potentials. In addition to the electrostatic interactions, the nonelectrostatic interactions of nonlipid molecules are modeled as hard spheres.

Electrostatic interactions were calculated by the MMM2D method which converts the charge interaction in the 2D periodic system (two, 2D membranes separated by a finite distance) to a

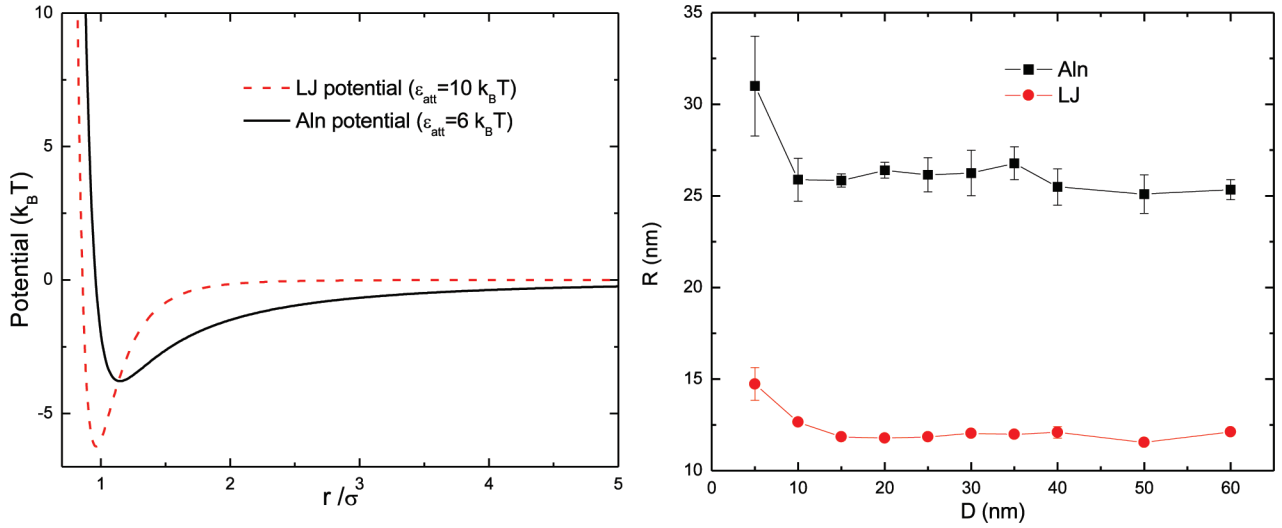

Figure 2. (a) Comparison of Lennard-Jones and Aln potentials. ε_{att} is 10 k_BT for LJ and 6 k_BT for Aln, and ε_{rep} is 4 k_BT for both. The x-axis is normalized by the soft-core radius, $\sigma/2$, associated with the lipid particles, and is 7 Å. (b) Average domain size R is plotted as a function of the intersurface separation, D, for the short-ranged lipid potentials shown in (a). The Aln model results in domains that are twice as large as those predicted by the LJ model. The domain size increases for small values of $D \sim 10$ nm, but for larger values of D, the domain size remains fairly constant.

rapidly converging series.[20] We treat water and the membrane as a uniform dielectric media with dielectric constant $\varepsilon = 79$. For simplicity, we neglect the finite dielectric contrast and assume that the electric field is nonzero only in the aqueous phase.

One problem in the simulations is that particles within a domain are bound by strong, short-range attractions and therefore move slowly. This means that a huge amount of simulation time is needed to properly sample the system under thermodynamic conditions. We accelerate this process by adding trial steps of global exchange of different types of surface particles and the cluster movement steps. Two types of the global exchange steps are considered: One exchanges particles randomly, and the other exchanges particles that are located near domain interfaces. In addition, three types of cluster movements were considered: One is a cluster movement of a single species (lipids), and the second is a cluster movement of two nearby species (lipid and surface charges). In addition, we allow for cluster movement of multiple domains. We emphasize that detailed balance must be obeyed before and after these trial moves, and there must be enough time between cluster moves so that the individual particles readjust in response to the new configuration.

In the simulations, the clusters are renewed every 5000 steps and the simulation is run for $4 \times 10^5 - 10^6$ steps. Our criterion for reaching equilibrium is related to the number of clusters. If total number of clusters remains stable for 10^5 steps, we consider that the system is in equilibrium; we then begin the data production steps. For the results shown here, three simulations were repeated for each parameter set.

RESULTS

System and Assumptions. In the initial stages of the simulation, positive surface charges (lipids in our model) aggregate due to the attractive hydrophobic interaction until the energetic cost of the electrostatic repulsion of lipids balances their cohesion energy; compared with infinite domains, the line energy of finite-size domains is increased but their electrostatic energy is decreased. Once the equilibrium domain size is reached, the domains remain roughly constant in size with small fluctuations at the boundaries. The domains diffuse slowly and change only near their boundaries. Global exchange steps and cluster moves help the system to evolve more efficiently. We repeated the simulation three times for each parameter set and found that the variations of the measured, average domain size or pressure presented in the results were small.

Our simulations have two major simplifications: the first one is that the lipid chain is represented by a single spherical particle, and the net electrostatic interaction and nonelectrostatic interactions are determined by the average intermolecular spacing. The other simplification is that we do not self-consistently calculate the effects of charge regulation on our system. The bare surface charge density used in the simulations is much larger than the measured, regulated effective surface charge density. However, the effective surface charge densities are often measured using surface forces and are extrapolated from the Debye−Huckel regime. This typically substantially underestimates the surface charge by 10−100 for millimolar salt concentrations. We describe this in more detail in the Appendix. We model the nonelectrostatic interactions of hydrophobic chains by potentials that depend only on the average intermolecular spacing; real lipid systems have additional degrees of freedom. To partially remedy this shortcoming, we consider our potentials as describing *effective* interactions between the lipids. Two types of such effective short-ranged simplification interactions (LJ and Aln) were used to mimic the hydrophobic properties.

To highlight the contrast between them, we used different values of ε_{att}. In Figure 2a, the LJ potential with $\varepsilon_{att} = 10\ k_BT$ and the Aln potential with $\varepsilon_{att} = 6\ k_BT$ are plotted. The repulsive part is taken to be identical: $\varepsilon_{rep} = 4\ k_BT$ for both. As seen in the figure, the LJ potential has a deeper energy minimum and a narrower attractive well compared with the Aln potential, which has a broader and shallower attractive well. Figure 2b shows that larger domains are formed for Aln potential than for LJ potential. The inverse screening length κ^{-1}, which varies with the inverse square root of the salt concentration, is chosen as 1000 Å, appropriate to pure water at a pH of 5. The number density of bare surface

dx.doi.org/10.1021/la1050282 |*Langmuir* 2011, 27, 4439–4446

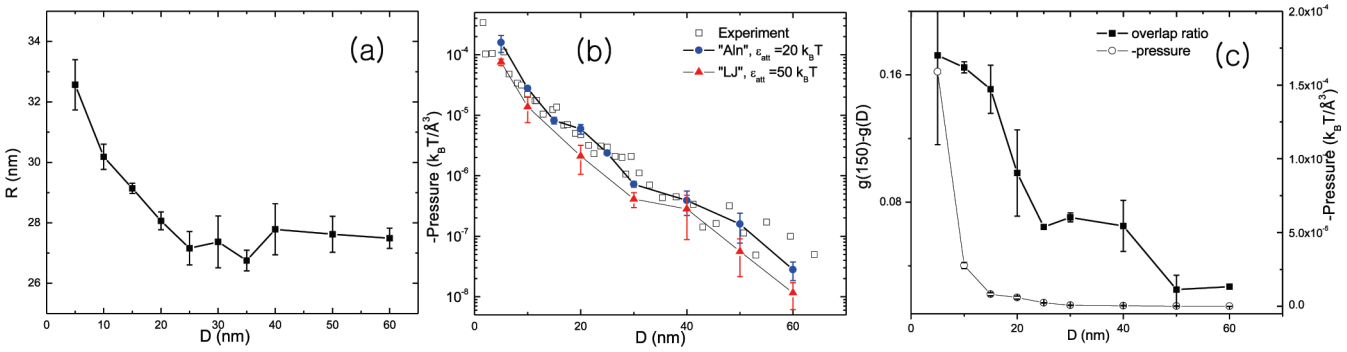

Figure 3. (a) Domain size, R, plotted as a function of the separation, D, between the two surfaces. It decreases sharply for small values of $D \leq 25$ nm but remains fairly constant for larger values of D. In particular, when $R > 30$ nm our simulations showed that a single domain was formed, suggesting a phase transition to macroscopic phase separation between the two charged species. (b) Pressure ratio plotted as a function of separation, D. Here $-P$ is plotted; i.e., the pressure is attractive. For the Aln model with $\varepsilon_{att} = 20\ k_BT$, the numerical results show good agreement with the experimental data. Agreement of the simulation and the experiment requires a value of $\varepsilon_{att} = 50\ k_BT$ for the LJ model. (c) Overlap ratio and pressure shown as a function of separation, D. Since the value of $g(\infty)$ is not universal and depends on the system conditions, we normalize the overlap to its value at a very large surface separation. The left axis is $g(150) - g(D)$, which is the difference in the overlap ratio defined in the text at separation of D compared with very large separations (of 150 nm) to very long separation. The two curves show a similar trend as a function of the distance. The lines are a guide to the eye.

charge is taken as $\sim$0.33 nm^{-2}. Mica is known to have a surface charge density of 1.8 e/nm^2 when it is fully charged. However, charge regulation effects tend to reduce the surface charge. The charging ratio is determined by the concentration of charged particles, the pH, and the dielectric constant of the solvent (among other effects), but in general, we seldom expect the surface to be fully charged under normal conditions. In this study 0.33 e/nm^2 is chosen as the overall surface charge density, since we did not find measurably strong attractions below this surface charge density. However, it is worth mentioning that recent experimental studies of uniformly charged mica with no additional species reported that the regulated effective surface charge density of bare mica is much smaller, around 0.015 e/nm^2.[21]

Comparison with Experiment. The Gouy−Chapman length ($\equiv 1/2\pi q l_B \sigma_s$) that corresponds to the parameters mentioned above is about 7 Å. The hard-core radius of the negatively charged surface particle is taken to 6 Å, and the LJ radius, $\sigma_s/2$, of the positive surface particle is taken to be 7 Å. While this is somewhat arbitrary, the actual sizes may indeed be different in a given experiment. The simulations model the aqueous phase as containing monovalent salt with a hard-core repulsive diameter of σ = 5 Å. The size of the system periodic boundary is about 87.2 nm; this allows us to simulate 5000 surface particles. The domain size, R, of the patchy charged surface is inversely proportional to the first moment of the scattering structure factor, $S(k)$[22]

$$R = 2\pi/k_{ave} \tag{2}$$

where

$$k_{ave} = \frac{\int_{k=0}^{k_{max}} kS(k)}{\int_{k=0}^{k_{max}} S(k)}$$

We find that the Aln potential results in larger domains as well as higher attractive pressures between two opposing patchy charged surfaces. This result indicates that the width of the attractive well of the potential plays an important role in determining the nature of the patchy charged domain. We also note that Aln potential allows the system to evolve, diffuse, and hence reach equilibrium faster than the LJ potential. In fact, this efficiency makes the simulation much faster, and thus we emphasize results obtained using the Aln potential.

The net pressure between the charged surfaces is calculated by statistically averaging

$$P = P_{en} + P_{el} + P_{col}$$

where P_{en} is the entropic pressure due to the salt, P_{el} is the electrostatic pressure at the midplane of two membranes, and P_{col} is a hard-core interaction pressure due to the finite size of salt particles. The electrostatic contribution is dominant and gives rise to the attraction between the charged surfaces. The contributions from P_{el} and P_{col} are zero when the salt concentration is zero and remain small for low salt concentrations.

Meyer et al.[8] measured the long-range nature of the attraction between two patchy membranes. They showed clear evidence of the formation of large, similarly charged domains on the mica surface via AFM image. From the AFM images, we estimate the domain sizes in the range of several tens to hundreds of nanometers. In this section, we show that our simulations can reproduce the long-range attractive pressure seen in the experiments and relate this to the nature of the finite charged domains.

In Figure 3b, we reproduce the experimental results of Meyer et al.[8] showing the long-range attraction between two patchy membranes as a function of their separation. We also show the simulation results that are in good agreement with the experiment. In Figure 3, the domain size is plotted as a function of the distance between the two patchy charged surfaces. The simulation conditions are the same as that of Figure 2b. Although the line tension is not explicitly calculated in our simulations, the trend in surface energy of the domains, which increases with the domain area ($\sim R^2$), can also be inferred. The radius is measured by eq 2.

We use the molecular scale attraction of the tails for the Aln potential, ε_{att}, as a parameter that allows us to fit the simulation results to the experiments. When $\varepsilon_{att} = 20\ k_BT$, the pressure fits the experimental results fairly well. If instead we consider the LJ potential, a fit of the simulation to the experiment requires a much stronger molecular attraction of $\varepsilon_{att} = 50\ k_BT$ as seen in Figure 3b. In our simulations, each positively charged surface particle contains one negative surface charge and two positive

dx.doi.org/10.1021/la1050282 |Langmuir 2011, 27, 4439–4446

lipid molecules; our simulations do not model the solvent explicitly and account for the solvent via the dielectric constant of water. Although we model the interaction between the effective lipid chains with a point particle potential that varies as $1/r^6$, the actual interactions of chains with several CH groups are longer ranged and stronger. This may explain the reason why the Aln gives better results than the LJ model.

We note that these interactions operate at the molecular level within a given surface; the attractive pressure measured in the experiments and calculated in our simulations is the global attraction of two oppositely charged surfaces and arises from the electrostatic interactions of their anticorrelated charged domains. The attractive pressure between two opposing patchy charged surfaces is relatively small for large spacings, larger than ∼20 nm; beyond this distance, the pressure is still negative but the magnitude is very small. We found that the attractions between the surfaces are still measurable at distances around ∼60 nm; beyond this distance, the pressure drops below our numerical precision. Since the hard-core osmotic pressure due to the excluded volume interactions of the salt is much smaller than the electrostatic pressure, it is clear that the primary reason for the attraction is the correlation of charge patches in two membranes.

It is of interest to see how the attraction depends on the domain size, the domain compactness (or the density of lipids in the domain), and the correlation between domains. The electrostatic anticorrelations between domains on opposing surfaces is the origin of the attractive pressure. To quantify the anticorrelation between domains, we introduce the overlap ratio, $g(z)$, between domains, defined as the ratio between the total number of particles and the number of particles in the upper plane of one charge type that overlaps particles in the lower plane of the same charge type when the separation of the planes is z. If the domains on the two opposing surfaces are perfectly anticorrelated, the charged domains in each plane are distributed in an alternating manner, and the overlap ratio would then be zero since no charge is opposite to one of the same species. On the contrary, if the domains on two opposite surfaces are weakly correlated, the overlap ratio increases and oppositely charged domains in the two opposing surfaces hardly recognize each other. To find a reference value for the zero-correlation limit, we consider a tentative value of large separation when the distance is 150 nm. The overlap ratio for this separation is about 0.38 when $\varepsilon_{att} = 20$ k_BT. There is a jump in the overlap ratio when the distance between surfaces is of the order of 20 nm, and the ratio slowly increases as the surface separation is decreased.

Small values of the overlap ratio indicate stronger correlations between oppositely charged domains between the two surfaces. However, the overlap ratio does not decrease in a manner that is similar to the decrease of the pressure when the distance between surfaces is increased, as can be seen in Figure 3c. The attraction decreases quickly with a nearly exponential decay, while the overlap ratio decreases in an approximately linear manner. From ref 5, the pressure depends on the effective domain size, which may be linearly dependent on the overlap ratio. The reason that the pressure decays faster than the overlap ratio may be because the pressure depends not only the correlation of the finite domains but also on the screening by salt in the bulk. For larger separations, this ratio quickly converges to the reference value of very large spacings. Interestingly, the sharp change happens when the distance is comparable to the domain size. This is probably because, at this distance scale, the interaction between charged domains in two opposing surfaces is comparable to the interaction between domains within a single plane. This result is consistent with the theoretical predictions for the zero salt limit.[5]

Larger domains are found (in the range of ∼5−∼20 nm). For small separations, the electrostatic correlation between oppositely charged particles (anticorrelation of the charge) in the two opposing surfaces reduces the free energy of the system and enhances the growth of the domains. The domains grow as the separation is decreased, until $D \sim 5$ nm, at which a single domain is seen in the simulations; this might be an indication of a phase transition from patchy charged surfaces to surfaces with macroscopic phase separation of the two charged species. Such a transition might correspond to the findings in ref 5 that predict the possibility of the first-order transition for zero salt; this transition arises from the interlayer interactions and is not predicted for a single surface. However, since our simulations are performed for a finite-sized periodic cell, our results may only suggest the possibility of such a phase transition. When $D >$ 25 nm, the change in size of the charged domains as a function of separation is smaller than the numerical fluctuations. We cannot observe the dependence within our numerical resolution in this regime. For larger intersurface separations, the domain size is more sensitive to the salt concentration and the surface tension (rather than to the separation) as indicated in ref 6.

It is worthwhile to mention that the simulations predict a domain size at large separations of ∼25−30 nm which is smaller than the experimental value of about 50 nm. One of the main reasons for this is the numerical limitation of the simulation that allows to treat only small numbers of particles; for example, we use 2500 particles for each surface. If domain size is in the range of about 30 nm, there are only a few domains on each surface, each of which contains about 1000 charged particles. Since we use periodic boundary conditions, there is an artificially strong electrostatic repulsion between similarly charged domains which is amplified as the domain size is increased. This long-range repulsion that arises from the periodic boundary conditions prevents the growth of the domains. The best way to overcome this artifact is to simulate a larger number of particles in a larger periodic cell, an approach that is currently limited by computational power. Although the simulated domain size is smaller than the experimental size by ∼40%, the simulated attractive pressure and its dependence on the intersurface separation agree remarkably well with experiment. This is perhaps because the pressure is more sensitive to the correlations and the charge density within the finite domain as opposed to the domain size.

Salt Concentration and Line Tension. We now discuss the dependence of the domain size on the salt concentration and line tension. In Figure 4a, the domain size is plotted as a function of the separation for different values of ε_{att} which controls the line tension between the lipid and mica domains. We find that the domain size depends only weakly on the value ε_{att}. Larger domains are found for higher values of ε_{att} which is consistent with theoretical predictions.[6] The physics behind this is related to the fact that in the absence of electrostatic interactions, positive line tension results in infinitely large domains—i.e., macroscopic phase separation. The attraction of two macroscopically phase-separated domains shows a slower decay (as the surface spacing is increased) than that of finite domains. For macroscopic phase separation, the attraction is that of two infinite, oppositely charged surfaces where according to ref 5 the attraction depends on distance as $\mathrm{sech}^2(\kappa D)$. In Figure 4b the pressure is shown as a function of the intersurface separation for different values of the

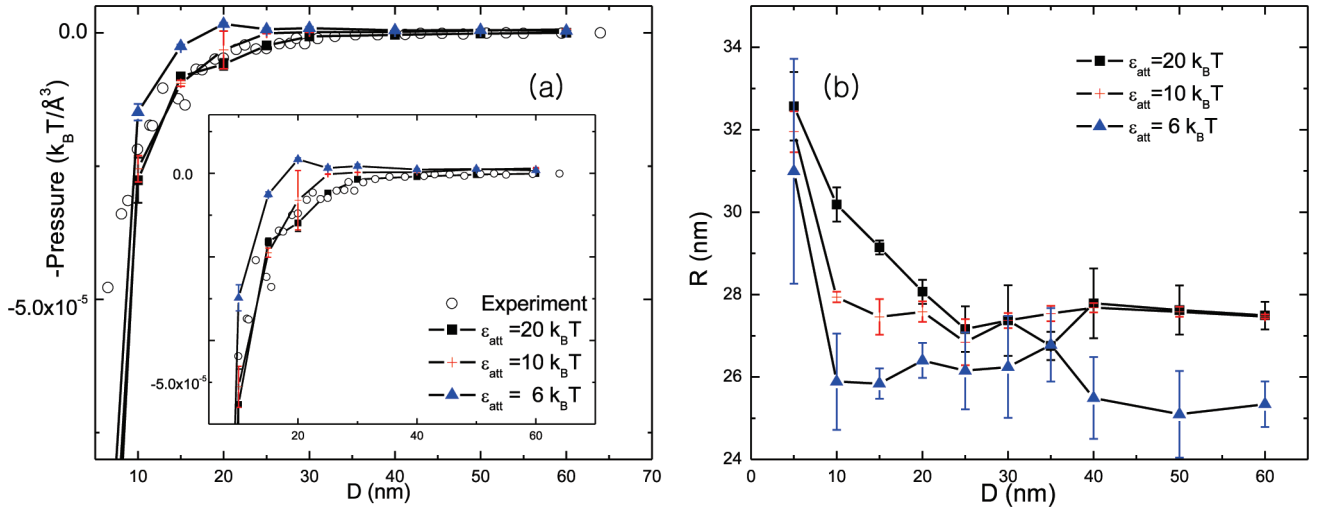

Figure 4. (a) Domain size plotted as a function of the intersurface separation, D, for three different values of the molecular lipid attraction ε_{att}. For higher values of ε_{att}, larger domains are formed. Inset is an enlargement of the figure. (b) Stronger attractive pressure is observed for higher values of ε_{att}. In particular, when ε_{att} = 6 k_BT or 10 k_BT, the pressure is attractive in the range of D = 20 or 30 nm.

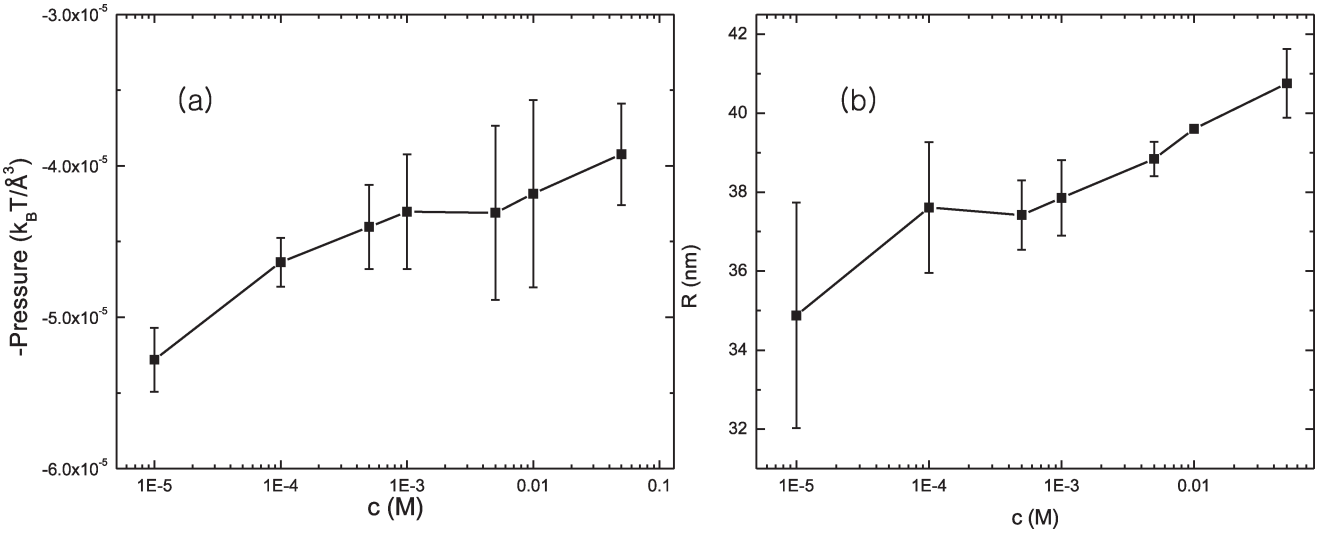

Figure 5. (a) Domain size for different salt concentrations given in M. Adding more salt increases the domain size, R. (b) Corresponding pressure as a function of salt concentration. The attraction is reduced for higher salt concentration.

molecular lipid attractive interactions (corresponding to the line tension). A higher value of the attractive pressure between surfaces is found for larger values of ε_{att}. The effect of the molecular attraction on the pressure is seen more clearly than its effect on the domain size. In particular, when $\varepsilon_{att} \leq 10\ k_BT$, there was no attraction between the two opposing surfaces for large separations. A reason for this is related to the fact that the actual equilibrium distance between lipids (i.e., their local packing density) is controlled by the value ε_{att}. For example, when D = 5 nm, the interlipid distance in the same domain is 1.502 ± 0.020 nm for $\varepsilon_{att} = 6\ k_BT$, 1.419 ± 0.001 nm for $\varepsilon_{att} = 10\ k_BT$, and 1.364 ± 0.026 nm for $\varepsilon_{att} = 20\ k_BT$. It is worthwhile to note that the interlipid distance not only depends on the interaction between lipids but also is known to depend on the charge asymmetry of the lipids and the separation between the surface.[23]

Analytical treatments of this problem predict that salt can enhance the domain size since it screens the electrostatic repulsion between lipids.[5,6] To observe this phenomena clearly in our simulations, we reduced the surface charge density by a factor of 2: i.e., 0.165 e/nm^2. This yields larger domains with same overall number of simulation particles. The system size for this simulation is 123.4 nm for 2500 surface charges on each surface. Since the charged domain contains hundreds of charged particles in its interior, the salt ions of one type are highly condensed on domains with the opposite local surface charge, thus reducing the electrostatic repulsions between lipids and thus increasing the domain size. We recall that the electrostatic repulsion of similarly charged particles within a domain is necessary to get finite domains in equilibrium; the electrostatic repulsion balances the positive line tension which favors large or even infinite domains. We obtain the same trend in our simulation results for the domain size as a function of salt concentration as shown in Figure 5b. It should be noted that a larger domain size does not necessarily imply a larger attractive interaction

dx.doi.org/10.1021/la1050282 |*Langmuir* 2011, 27, 4439–4446

between the two surfaces for all conditions, as seen in Figure 5a. This is because the intersurface interaction is reduced by the screening effect of the salt, despite the fact the anticorrelated domains are larger in size for higher salt concentration. The high charge density within the domains (for example, the local charge density when $\varepsilon_{att} = 20\ k_BT$ is about 0.42 e/nm^2) induces a relatively large number of counterions—compared with DH theory—to be near the surface, and this screens the interactions between the surfaces. In addition, we study the effect of reducing the surface charge density compared with the simulations shown in Figure 3. The domain size for a surface charge density of 0.165 e/nm^2 increases by 15% compared with the bare surface charge density of 0.33 e/nm^2, but the pressure is also reduced by 61%.

DISCUSSION

Our simulations show that heterogeneously charged membranes with mobile charges have finite-sized domains whose anticorrelation in charge lead to a relatively long-ranged attraction for intersurface separations in the range of several tens of nanometers. This distance is relevant to some biological situations; for example, the separation between vesicles containing SNARE proteins and the plasma membrane of the cell is around a few tens of nanometers when fusion is observed, and the interdistance between microtubules is similar. The finite sizes of the domains are determined by the balance of the hydrophobic attraction of the lipids with the electrostatic repulsions of the surface charges. For small separation distances of a few nanometers, the correlations play an important role in controlling both the domain size and the intersurface attractive pressure. Larger correlation gives rise to larger domains and stronger attraction. We note that the bare surface charge density of 0.33 e/nm^2 is much larger than the effective surface charge density of 0.015 e/nm^2.[21] Future studies might focus on a self-consistent calculation of the effective surface charge density due to charge regulation in these systems.

For smaller intersurface separations, the domain size and the negative pressure increase, while the overlap ratio decreases, and a sharp jump is found near 20 nm separation. For larger separations, D, the domain size depends less sensitively on D. Instead, the domain size is more sensitive to the short-ranged interaction and salt concentration similar to the case of a single surface with two charge species. For large values of D, $\sim$ 50 nm, the attraction drops to almost zero and the overlap ratio levels off to maximum. In this regime, the pressure follows the domain size but the correlation between domains (overlap ratio), the lipid concentration in domain, and salt are other important factors that determine the intersurface attractive pressure.

We find that a higher density of lipid particles is found in a single domain with a higher line tension for larger values of the molecular lipid attraction ε_{att}. Higher values of ε_{att} not only increase the domain size but also increase the lipid density within a domain; i.e., the interlipid distance within a domain decreases. The pressure is quite sensitive to these effects. For the case of small values of $\varepsilon_{att} = 6-10\ k_BT$, we could not find any attractions for intersurface distances beyond 20 nm.

Salt typically screens the electrostatic potential and reduces electrostatic interactions. Theoretical studies of intersurface attractions in patchy domain systems[5] predict that salt reduces the electrostatic repulsion between like charges and increases the domain size. Our simulations agree with these theoretical predictions. However, the same theories also predict that in the strong-screening, Debye−Huckel regime, the larger domain size is obtained as the salt concentration is increased, dominating the screening effect of added salt, so that the intersurface attractive pressure increases with salt. Our simulations show the contrary: in contrast to the increase of the domain size, the pressure decreases as salt is added. Whether this is due to the strong screening assumption of the linearized theory compared with our relatively highly charged surfaces remains to be seen. However, in our simulation range, salt plays its traditional role.

APPENDIX

The effective surface charge density measured in the experiment is much smaller than the bare charge density we used in the simulation. However, it is natural for the highly charged surfaces like our system. If $\sigma_s \sim 1\ nm^{-2}$, then the Gouy−Chapman length $\lambda \equiv 1/(2\pi l_B \sigma_s) \approx 3$. For added 1−1 salt, which means both the positive and negative ions are monovalent, the Debye length is of order 100 Å for 1 mM salt. So, for $c_s \leq 1$ M, $\kappa\lambda < 1$, where $\kappa^2 \equiv 8\pi c_s l_B$.

At large distance from the surface ($x \gg \lambda$), the electrostatic potential has the Debye−Huckel form $\varphi(x) = \varphi_0 e^{-\kappa x}$. We assume that the force measurements in the experiment are made in this regime.

At the Poisson−Boltzmann level and for no salt, the counterions density varies as

$$\rho(x) = \frac{1}{2\pi l_B}\frac{1}{(\lambda + x)^2} \tag{3}$$

We assume that the effect of co-ion is much smaller near the strongly charged surface.

At a distance ξ, such that

$$\rho(x) = c_s \tag{4}$$

we expect crossover to DH behavior

$$\xi = \frac{2}{\kappa}\left(1 - \frac{1}{2}\kappa\lambda\right) \tag{5}$$

from the above equations. At $x = \xi$, where the DH form becomes valid, the effective surface charge density is

$$\sigma_{eff} = \sigma_s - \int_0^{\xi} \rho(x)\, dx \approx \frac{\kappa}{4\pi l_B} \tag{6}$$

Then

$$\frac{\sigma_{eff}}{\sigma_s} \approx \frac{1}{2}\kappa\lambda \ll 1 \tag{7}$$

So, it is not strange that the effective surface charge density is much smaller than the bare surface charge density in our system.

AUTHOR INFORMATION

Corresponding Author

*E-mail yongseokjho@gmail.com.

ACKNOWLEDGMENT

S.A.S. and P.A.P. are grateful to the U.S.−Israel Binational Science Foundation for their support. S.A.S. thanks the Perlman Family Foundation for its historical generosity and partial support. P.A.P. was supported by the WCU (World Class

University) program through the National Research Foundation of Korea funded by the Ministry of Education, Science and Technology No. R33-2008-000-10163-0 and the National Science Foundation Grant NSF-DMR 0803103. This work was partially supported by the IMI Program of the National Science Foundation under Award No. DMR04-09848. The calculations were performed using the SGI Altix3700Bx2 at the Advanced Fluid Information Research Center, Institute of Fluid Science, Tohoku University.

REFERENCES

(1) Simons, K.; Toomre, D. *Nat. Rev. Mol. Cell Biol.* **2000**, *1*, 31–39.
(2) Loverde, S.; Velichko, Y.; de la Cruz, M. *J. Chem. Phys.* **2006**, *124*, 144702.
(3) Cruz, M. *Soft Matter* **2008**, *4*, 1735–1739.
(4) Lukatsky, D.; Shakhnovich, B.; Mintseris, J.; Shakhnovich, E. *J. Mol. Biol.* **2007**, *365*, 1596–1606.
(5) Brewster, R.; Pincus, P.; Safran, S. *Phys. Rev. Lett.* **2008**, *101*, 128101.
(6) Naydenov, A.; Pincus, P.; Safran, S. *Langmuir* **2007**, *23*, 12016–12023.
(7) Landy, J. *Phys. Rev. E* **2010**, *81*, 11401.
(8) Meyer, E.; Lin, Q.; Hassenkam, T.; Oroudjev, E.; Israelachvili, J. *Proc. Natl. Acad. Sci. U.S.A.* **2005**, *102*, 6839.
(9) Perkin, S.; Kampf, N.; Klein, J. *Phys. Rev. Lett.* **2006**, *96*, 38301.
(10) Perkin, S.; Kampf, N.; Klein, J. *J. Phys. Chem.* **2005**, *109*, 3832–3837.
(11) Solis, F.; Stupp, S.; de La Cruz, M. *J. Chem. Phys.* **2005**, *122*, 054905.
(12) Frenkel, D.; Smit, B. *Understanding molecular simulation*; Academic Press, Inc.: Orlando, FL, 2001.
(13) Valleau, J.; Cohen, L. *J. Chem. Phys.* **1980**, *72*, 5935.
(14) Widom, B. *J. Chem. Phys.* **1963**, *39*, 2808.
(15) Shing, K.; Gubbins, K. *Mol. Phys.* **1982**, *46*, 1109–1128.
(16) Boulougouris, G.; Economou, I.; Theodorou, D. *Mol. Phys.* **1999**, *96*, 905–913.
(17) Parsonage, N. *Mol. Phys.* **1996**, *89*, 1133–1144.
(18) Jones, J. *Proc. R. Soc. London, Ser. A* **1924**, *106*, 463–477.
(19) Brannigan, G.; Brown, F. *J. Chem. Phys.* **2004**, *120*, 1059.
(20) Arnold, A.; Holm, C. *Comput. Phys. Commun.* **2002**, *148*, 327–348.
(21) Kampf, N.; Ben-Yaakov, D.; Andelman, D.; Safran, S.; Klein, J. *Phys. Rev. Lett.* **2009**, *103*, 118304.
(22) Nekovee, M.; Coveney, P.; Chen, H.; Boghosian, B. *Phys. Rev. E* **2000**, *62*, 8282–8294.
(23) Lau, A.; Pincus, P. *Eur. Phys. J. B* **1999**, *10*, 175–180.